Meteorol. Atmos. Phys. 51, 147–164 (1993)

Meteorology and Atmospheric Physics

551.589(98)

[1] Cooperative Institute for Research in Environmental Sciences, University of Colorado, Boulder, CO, U.S.A.
[2] Department of Atmospheric Sciences, University of Illinois, Urbana-Champaign, Urbana, IL, U.S.A.

Characteristics of Arctic Synoptic Activity, 1952–1989

M. C. Serreze[1], J. E. Box[1], R. G. Barry[1], and J. E. Walsh[2]

With 11 Figures

Received November 10, 1992
Revised December 20, 1992

Summary

Synoptic activity for the Arctic is examined for the period 1952–1989 using the National Meteorological Center sea level pressure data set. Winter cyclone activity is most common near Iceland, between Svalbard and Scandinavia, the Norwegian and Kara seas, Baffin Bay and the eastern Canadian Arctic Archipelago; the strongest systems are found in the Iceland and Norwegian seas. Mean cyclone tracks, prepared for 1975–1989, confirm that winter cyclones most frequently enter the Arctic from the Norwegian and Barents seas. Winter anticyclones are most frequent and strongest over Siberia and Alaska/Yukon, with additional frequency maxima of weaker systems found over the central Arctic Ocean and Greenland.

During summer, cyclonic activity remains common in the same regions as observed for winter, but increases over Siberia, the Canadian Arctic Archipelago and the Central Arctic, related to cyclogenesis over northern parts of Eurasia and North America. Eurasian cyclones tend to enter the Arctic Ocean from the Laptev Sea eastward to the Chukchi Sea, augmenting the influx of systems from the Norwegian and Barents seas. The Siberian and Alaska/Yukon anticyclone centers disappear, with anticyclone maxima forming over the Kara, Laptev, East Siberian and Beaufort seas, and southeastward across Canada. Summer cyclones and anticyclones exhibit little regional variability in mean central pressure, and are typically 5–10 mb weaker than their winter counterparts.

North of 65° N, cyclone and anticyclone activity peaks during summer, and is at a minimum during winter. Trends in cyclone and anticyclone activity north of 65 N are examined through least squares regression. Since 1952, significant positive trends are found for cyclone numbers during winter, spring and summer, and for anticyclone numbers during spring, summer and autumn.

1. Introduction

Until the early 1950s, considerable uncertainty existed concerning synoptic activity in the Arctic. As discussed by Jones (1987), this reflected the combined effects of sparse observational data, coupled with a theoretical view that the Arctic must be dominated by a more-or-less permanent anticyclonic cell. This concept, first put forth by Helmholtz (1888), was elaborated by Hobbs (1910, 1926), in his "glacial anticyclone" theory. He subsequently expanded this idea into his "Greenland glacial anticyclone" theory, involving a persistent high pressure cell over the Greenland ice sheet that strongly influenced mid-latitude weather (Hobbs, 1945).

Although the "Greenland glacial anticyclone" theory was disproved from observational evidence (Loewe, 1936; Dorsey, 1945; Matthes, 1946; Matthes and Belmont, 1946), the idea of anticyclones as the dominant feature of the Arctic circulation persisted. Jones (1987) finds that sea level pressure (SLP) analyses from the U.S. Historical Weather Map Series away from the North Atlantic sector contained strong positive pressure biases (4–6 mb) up to 1930, and lesser errors up to 1939. Apparently, these maps were prepared during World War II by relatively untrained analysts extrapolating pressures into the data-poor Arctic with a "glacial anticyclone" concept still in mind (Jones, 1987). Even in the

early 1950s, most studies still showed cyclonic activity to be concentrated along the periphery of the Arctic (e.g., Pettersen, 1950; Rae, 1951), a view which may have been influenced by Sverdrup's (1933) observations during the "Maud" expedition (1918–1925). The notable dissenting view was that of Dzerdzeevskii (1945). Based on data from the Russian drifting icebreaker "Sedov", the drifting ice island "North Pole 1" and other high Arctic stations (Jones, 1987), he correctly concluded that cyclonic activity was also common in the central Arctic, especially in summer.

Through the 1950s, data from Russian and U.S. drifting stations (e.g., the North Pole stations and T3), began to be incorporated routinely into SLP analyses. These improved analyses provided the basis for a series of studies (e.g., Wilson, 1958; Hare and Orvig, 1958; Keegan, 1958; Namias, 1958; Reed and Kunkel, 1960) which form the framework for the modern view of the Arctic circulation. These studies showed that, while anticyclones are common and often persistent features of the Arctic circulation, especially in winter and over land areas, cyclones are also very frequent and depending on the season, may be found anywhere in the Arctic.

More recently, Bradley and England (1979) provide a synoptic climatology of the Canadian Arctic for 1947–1974. Overland and Pease (1982) examine 23 years of winter cyclone activity in the Bering Sea, while Gorshkov (1983) provides a climatology of Arctic highs and lows and system tracks based on unspecified Soviet data up to about 1980. LeDrew (1983, 1984, 1987) and LeDrew et al. (1991) have examined the dynamics of synoptic development through extensive case studies, while Serreze and Barry (1988) analyzed Arctic cyclone and anticyclone characteristics above 70° N for 1979–85, using improved pressure analyses that incorporate data from arrays of buoys drifting with the pack ice cover (Thorndike and Colony, 1980). Information on Arctic synoptic activity is also provided by Bell and Bosart (1989) who report on a 15-year analysis of 500 mb closed cyclone and anticyclone centers up to 82° N, and Whittaker and Horn (1984), who provide summaries of northern hemisphere cyclone activity, cyclone tracks and principal regions of cyclogenesis, based a 20-year record compiled from several different sources.

Several issues, however, point toward the need for a long-term analysis of synoptic activity specific to the Arctic. First, while General Circulation Models (GCMs) indicate that the Arctic is a region where the effects of greenhouse warming may be first detected and most pronounced (Hansen and Lebedeff, 1987; Schlesinger, 1988; Washington and Meehl, 1989; Cubasch and Cess, 1990), model-predicted temperature increases during the next century may be indistinguishable from those related to natural variability in the Arctic circulation (Walsh and Chapman, 1990). Furthermore, the "transient" greenhouse response may not be reflected as a general increase in temperature, but increased climatic variability. A long-term analysis of Arctic cyclone and anticyclone activity can provide an assessment of present circulation variability, as well as an indication of whether trends in synoptic activity already exist.

Second, GCMs differ substantially in their inherent natural variability and their depiction of even basic fields for the current climate of the Arctic (Walsh and Crane, 1992) raising concern as to the integrity of their response to a change in forcing and their ability to simulate realistically future climatic states. Accurate simulation of the SLP field is especially important, as the circulation of the Arctic sea ice cover is strongly wind driven (Fig. 1). Wind-driven variability in the ice motion field is associated with changes in regional ice extent (e.g., Walsh and Johnson, 1979), ice compactness (Serreze et al., 1989) and freshwater input into the North Atlantic (Dickson et al., 1988), with possible atmospheric feedbacks. As variability in the SLP field is strongly influenced by the frequency, strength and migration of pressure systems, the ability of GCMs to simulate accurately the present SLP distribution also depends on their ability to reproduce observed mean patterns of synoptic activity.

The present paper examines climatological patterns of Arctic synoptic activity for the period January 1952 through June 1989. Climatological distributions of Arctic cyclones and anticyclones, system mean central pressures, and relationships between mean SLP fields are analyzed for winter (December–February) and summer (June–August). Mean winter and summer cyclone tracks are examined using a 15-year (1975–1989) subset of this record. The annual cycle of synoptic activity for the Arctic north of 65° N is addressed, and

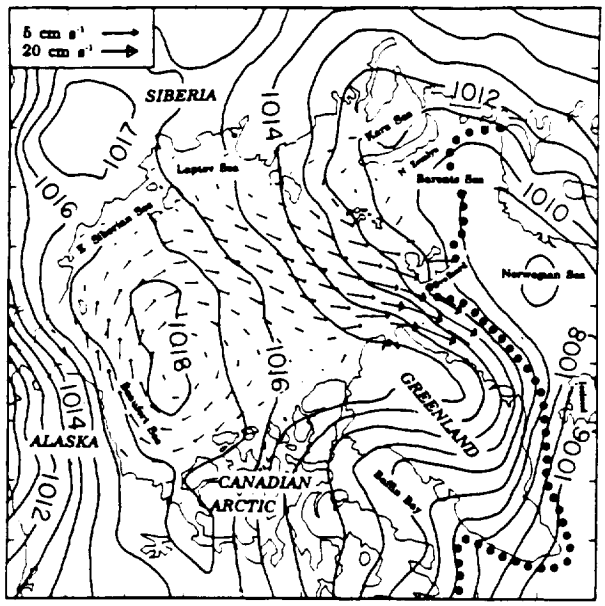

Fig. 1. Location map of the Arctic showing geographic locations, and mean annual fields of sea level pressure (mb) (1952–1989, from NMC), and sea ice circulation (ice motion vectors from unpublished data provided by R. Colony, Polar Science Center, Univ. Wash., Seattle), and the approximate mean maximum winter sea ice boundary (dotted line)

seasonal time series of cyclone and anticyclone occurrence and mean central pressures are examined for trends. As compared to our earlier paper (Serreze and Barry, 1988) the present study examines a much larger area, allowing for a more comprehensive assessment of patterns and variability in synoptic activity, and presents a more quantitative assessment of cyclone tracks. To our knowledge, our paper also represents the first attempt to identify trends in Arctic synoptic activity.

2. Data and Techniques

2.1 SLP Analyses

Our primary data source is a record of the position and central pressure of cyclone and anticyclone centers, obtained through application of an automated detection algorithm to the historical National Meteorological Center (NMC) SLP data set in the Octagonal Grid format. This data set, obtained in CD-ROM format from University of Washington, (Mass and Edmon, 1987) represents a blend of the U.S. Navy Northern Hemisphere SLP set (1952–1962), and NMC final analyses (1963–1989), which represent the initialization fields for NMC's prediction models.

We are aware of the possibility of less accurate analyses during the early part of the record, especially over the Arctic Ocean. As discussed, SLP data over the central Arctic Ocean were known to be seriously in error until the late 1930s (errors were also apparent over land areas, see Trenberth and Paolino, 1980), but by the early 1950s, data from typically 2–3 drifting stations at a time began reporting on a regular basis (Hastings, 1971), considerably improving the quality of the analyses over the ocean. Since 1979, data from arrays of drifting buoys from the Arctic Ocean Buoy Program (AOBP) (Thorndike and Colony, 1980) have been incorporated into the NMC fields. Nevertheless, the NMC analysis procedures have undergone numerous changes through the years (Trenberth and Olson, 1988); we are not aware of any assessments of the earlier U.S. Navy map series or of comparisons between the NMC and U.S. Navy fields. Possible temporal and spatial inhomogeneities in the data set should be kept in mind when interpreting our results, especially those regarding time series of synoptic activity (section 4).

2.2 Detection Algorithm

Our detection algorithm makes use of the daily pressure arrays at 1200 UTC for the 21 × 21 subsection of the NMC grid centered over the pole in which the origin ($i = 1$, $j = 1$) is taken to be at the top left of the array. The decision to use 1200 UTC data only (as opposed to twice-daily analyses) was simply based on the need to reduce the data volume to a manageable size; in particular, manual tracking of system migration (see section 2.4) from twice daily data would have been extremely time consuming.

The grid array extends to approximately 55° N on each side. For detection of cyclones, pressures at all grids from $i = 4$ to $i = 18$ and $j = 4$ to $j = 18$ are tested to determine the difference in pressure with respect to each of the eight surrounding grid points. If the difference is at least 2 mb, the central point is identified as a cyclone center. If this condition is not satisfied, but none of the eight pressure values fall from the tested central value, the next surrounding "shell" of 12 points is

examined. If in each direction from the tested central point, the pressure at the immediately adjacent or the next outer grid point increases by at least 2 mb (with some special consideration of the diagonal directions), then the center point passes as a cyclone center. If, again, pressure does not fall, but increases by less than 2 mb, the third surrounding shell is tested in a similar fashion.

As we test from $i+/-3$ and $j+/-3$ away from each central point, the NMC grid array over which systems can be identified reduces to 15×15, which extends to approximately 65° N on each side and about 55° N at the corners. In our earlier study based on manual analysis of seven years of AOBP data (Serreze and Barry, 1988), systems could only be confidently identified above about 72° N, hence severely restricting the spatial scope of the analysis. Each NMC grid point in the Arctic is separated by approximately 400 km; thus the minimum diameter of systems that can be identified is about 800 km, and the maximum about 2400 km. For comparison, the grid spacing in the Arctic in current GCMs is typically of the order of 500 km (R15 spectral resolution), but in one version of the Geophysical Fluid Dynamics Laboratory (GFDL) model is about 250 km (Walsh and Crane, 1992).

Only systems with a central pressure < 1012 mb are counted as cyclones. As systems with broad centers are occasionally counted twice or more, the grid array is retested to determine whether any points adjacent to each other are defined as cyclone centers. If so, these are all considered duplicate centers of the same system. Outputs of the algorithm are the date, position and central pressure value (in mb) of each cyclone. For cyclones with duplicate centers, the position is taken as the average latitude and longitude of the duplicate centers.

The same techniques are used to detect anticyclones, except that pressures must fall from the tested central value by at least 1.5 mb. The lower threshold reflects the tendency for such systems to have broader centers than cyclones. The selection of 1.5 mb was subjectively based on the "best match" of comparisons between the algorithm output using different thresholds with manual analysis of system centers from pressure charts. We have compared our cyclone and anticyclone data bases to results from manual inspection of pressure maps, and find that the algorithm correctly identified system centers over 95% of the time.

2.3 *Spatial Analysis of System Frequencies*

To examine spatial patterns of synoptic activity, the latitude and longitude of each system center is first transformed into x and y values, using equations given by Thorndike and Colony (1980). This Cartesian coordinate system has its origin at the pole, with x increasing (in km) along the Greenwich meridian, and y increasing (in km) along the 90° E meridian. The rectangular region enclosing 65° N (i.e., the area enclosed by the 15×15 NMC grid subsection), also referenced to x, y coordinates, is then divided into a new 10×10 grid cell network. Grids cells are 556 km (5° of latitude) on a side, hence enclosing an area of approximately 309,000 km^2. Systems counts are simply tallied in each grid cell, converted into percent frequencies, and contoured.

This technique, used previously by Keegan (1958), Reed and Kunkel (1960) and in our previous study (Serreze and Barry, 1988), differs from that typically used in mid-latitudes (e.g., Zishka and Smith, 1980; Hayden, 1981a) in which system occurrences are first tallied in latitude/longitude boxes, with an area normalization applied to the raw counts to correct for convergence of the meridians. Hayden (1981b) notes that latitude-dependent adjustments, however, introduce their own biases. As convergence of the meridians is severe at high latitudes, the equal-area box approach is obviously better for the Arctic. However, Taylor (1986) points out that the frequency of cyclones in equal-area boxes can be influenced by the track orientation relative to the orientation of the grid cell; this influences the cell's effective cross section. Circular cells can be used to avoid this problem (Taylor, 1986), but in practice, the equal-area approach is considerably more straightforward. Nevertheless, for all techniques, the frequency values will tend to rise as the area of the grid box (or circle) increases. As different studies have used quite different cell areas (e.g., 260,000 km^2 by Keegan (1958) vs. 100,000 km^2 by Reed and Kunkel (1960), compared to 309,000 km^2 here), quantitative comparisons between these studies are difficult.

2.4 Cyclone Tracks

Using the record of system centers in conjunction with the daily MSL charts, individual cyclones have been tracked manually for winter and summer from January 1975 through June 1989. Obviously, this technique poses difficulties. For example, two separate systems occasionally merge into one, while single systems sometimes split in two. Edge-effect problems also occur, in that a system will migrate into the study region, then drop below the map edge. Occasional days are also missing from the SLP record. A series of rules was consequently adopted to account for these problems.

If two cyclones appear to merge into one, the system retains the number of that cyclone with the lower central pressure on the previous day. If one cyclone splits into two, the system with the lower central pressure retains the number of the original system, with the other considered to be new. When a missing day is encountered, all systems on the next available map are taken as new. While in many cases, it would have been possible to "carry over" a system from a missing day based on similarity of map patterns, we felt that re-numbering all systems would better avoid possible ambiguities in assessing daily cyclone motion. Nevertheless, for the 1975–1989 period, fewer that 3% of days were missing from the analyses.

Using the numbered catalogue, the daily displacements of each cyclone (in km) lasting two days and longer is determined, using the same x, y coordinate system discussed previously. The displacement observations are binned into the 10×10 array, and mean x and y vector components are computed for each cell. The gridding technique represents a conversion of the Lagrangian system position data into an approximation of the Eulerian velocity field. We also compute a "constancy" statistic (C) of cyclone motion for each grid box as $(V_r/V_s)^*100$, where V_r is the resultant vector magnitude and V_s is the mean scalar speed, both based on the total daily x and y displacement values in each grid box. For the extreme case of $C = 100$, all systems move in the same direction, while for $C = 0$, there is no preference in the direction of system migration.

3. Spatial Patterns of Synoptic Activity

3.1 Winter

Figure 2 shows the long-term spatial patterns of cyclone (a) and anticyclone (b) frequencies for winter. To accentuate regions with frequent

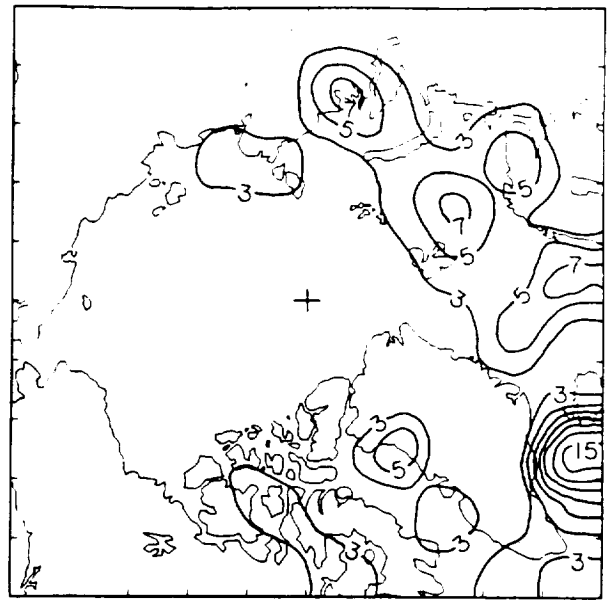

a

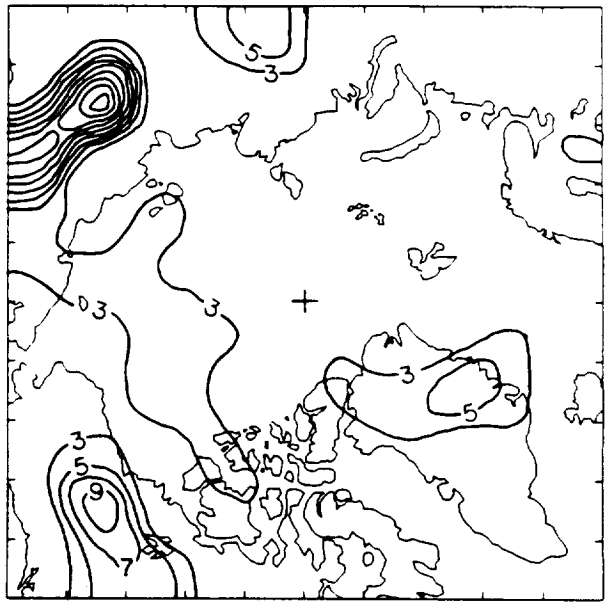

b

Fig. 2. Cyclone (a) and anticyclone (b) % frequencies for winter, 1952/53–1988/89 in squares of 306.000 km², for systems with central pressure < 1012 mb (cyclones) and > 1012 mb (anticyclones). A cutoff contour of 3% frequency is chosen to accentuate areas of frequent synoptic activity

synoptic activity, we use a 3% frequency cutoff for the contours, which corresponds to approximately 100 systems. The highest cyclone frequencies (> 15%) are found just south of Iceland, which corresponds to the well-known Icelandic Low. Another region of high frequencies is located over Baffin Bay (> 5%), with a third region found over the southern Canadian Arctic Archipelago (> 3%). Finally, the entire eastern Arctic Ocean is also characterized by high frequencies, with local maxima between Svalbard and Scandinavia (> 7%), and over the Norwegian and Kara seas (> 7%). Cyclones tend to be relatively uncommon over the central Arctic Ocean, Siberia and Alaska. Frequency maxima for anticyclones (Fig. 2b), are found over eastern Siberia (> 19%), corresponding to the well-known Siberian High, the Alaska/Yukon region (> 9%), Greenland and western Siberia (> 5%). A broad region of frequencies over 3% is also found in the Pacific side of the Arctic Ocean. A comparison between Figs. 2a and 2b shows that there is little overlap between frequency maxima of cyclones and anticyclones. These results agree well with those from earlier studies (e.g., Keegan, 1958; Gorshkov, 1983; Whittaker and Horn, 1984; Serreze and Barry, 1988).

Figure 3 shows that the mean central SLP of cyclones (a) and anticyclones (b) exhibit strong regional differences. While the region of highest cyclone frequencies is found near Iceland, these systems also tend to be deep (< 985 mb). Strong systems (< 985 mb) are also found over the Norwegian Sea and southwest of Greenland. Central pressures for individual systems in these regions are frequently lower than 970 mb, occasionally dropping below 950 mb. By contrast, those over the Barents and Kara seas, Baffin Bay and the Canadian Arctic Archipelago are relatively weak, with central pressures between 986 and 995 mb, and locally > 995 mb (Fig. 3a). Anticyclones associated with the Siberian, central Arctic Ocean and Alaska/Yukon frequency maxima tend to be strongest, with mean pressures > 1035 mb (Fig. 3b). By contrast, those found over Greenland are relatively weak (1025–1034 mb).

Siberian anticyclones form primarily in response to the strong radiative losses from the snow-covered land surface. They are typically associated with low tropospheric thicknesses (Keegan, 1958), although Bell and Bosart (1989) show that a

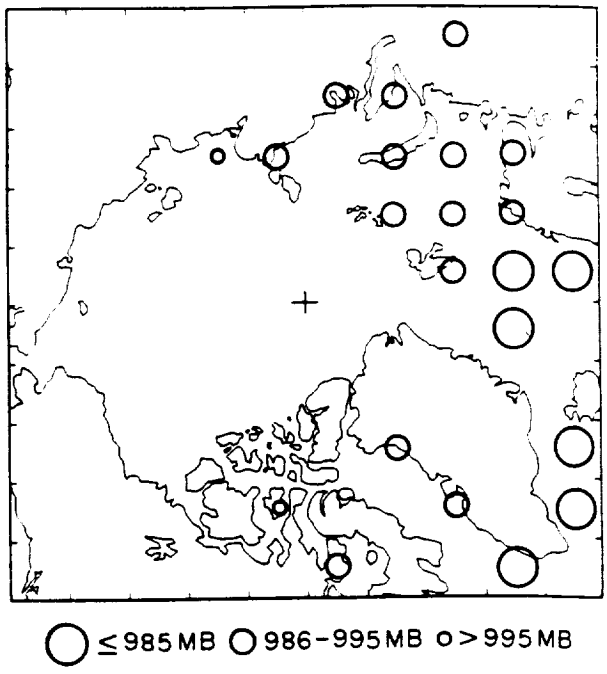

Fig. 3. Mean cyclone (a) and anticyclone (b) pressures (mb) for winter, 1952/53–1988/89 for grid cells with > 3% frequency of cyclones

closed anticyclonic circulation may occasionally be evident at 500 mb. While central pressures for individual Siberian anticyclones are often shown to exceed 1050 mb, pressures are likely often

overestimated in that station pressures are extrapolated to sea level using the local lower tropospheric temperature lapse rate, which, due to frequent low-level temperature inversions, will often yield a spuriously low sea level temperature (Walker, 1967). In this regard, we note that peak anticyclone activity is shown to occur near station Verkhoyansk (67.5° N, 133.4° E), located in the Yana river valley, which has the strongest wintertime temperature inversions in the Eurasian Arctic (Serreze et al., 1992) and is also recognized as the coldest location in Asia (Borisov, 1965).

According to Keegan (1958), anticyclones over the central Arctic Ocean tend to form as an extension of the Siberian High, with the Alaska/Yukon peak representing a mixture of cold systems associated with periods of extreme extension of the Siberian High, Pacific blocking highs associated with a warm ridge at 500 mb, and systems migrating from lower latitudes. A frequent occurrence of the second type is suggested from inspection of mean winter 500 mb height fields (e.g., Palmen and Newton, 1969), which show the axis of the mean North American ridge slightly west of the area of the frequency maximum. Nevertheless, individual systems are usually not closed at 500 mb (Bell and Bosart, 1989). The anticyclone peak over Greenland should be viewed with some suspicion; as has long been noted (e.g., Keegan, 1958; Putnins, 1970), this frequency maximum can also be biased by the effects of sea level correction. For a detailed discussion of the circulation over Greenland, the reader is referred to the study of Putnins (1970).

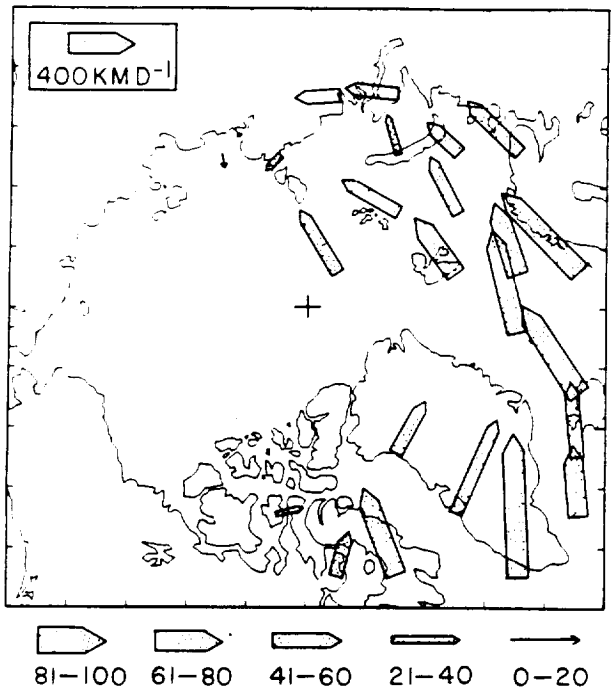

Fig. 4. Mean cyclone motion vectors for winter, 1975/76–1988/89. The length of each arrow is the mean vector magnitude, with the width proportional to the index of motion constancy, V_r/V_s (see text). Vectors are only plotted for grid cells with at least a 3% frequency of cyclones

The mean motion of winter cyclones is illustrated in Fig. 4. For clarity, vectors are only plotted for grid cells with at least a 3% frequency of cyclones. The deep eastern Arctic cyclones tend to track ENE. The width of the plotted vectors, which is proportional to the constancy of the cyclone motion, indicates that the general ENE motion of these systems is also quite consistent ($61\% < C < 80\%$). Both the resultant velocity and motion constancy of systems become smaller near the Kara Sea, which, coupled with the increase in mean cyclone pressures (Fig. 3a), is indicative of decaying systems. Systems near Baffin Bay tend to show a similar ENE motion, but with a more northerly component indicated for systems over Baffin Island.

Over the Arctic, these tracks agree well with those of Whittaker and Horn (1984). Their results show that winter cyclones over the eastern Arctic tend to originate in cyclogenetic zones along the mid-Atlantic seaboard, south and southeast of Newfoundland, near Svalbard and Scandinavia, as well as within an area of lee-side cyclogenesis east of southern Greenland. Orographic cyclogenesis is also recognized east of Iceland and along the western coast of Norway (U.K. Meteorological Office, 1964). Systems often intensify as they enter the Greenland and Norwegian seas, which in some cases is associated with systems drawing cold air from the central Arctic into their circulation (U.K. Meteorological Office, 1964). Consequently, we can interpret the cyclone frequency maximum in the eastern Arctic as reflecting a combined population of systems with remote origins in mid-latitudes, as well as those either generated or rejuvenated in response to more local conditions.

Whittaker and Horn (1984) also show that cyclones in Baffin Bay and the Canadian Arctic Archipelago tend to form in the cyclogenetic regions east of the Rocky Mountains in Alberta

and Colorado, with separate tracks converging in the Great Lakes region and then progressing northward, with a cyclogenetic region east of Labrador tending to produce new systems or regenerate old ones, which subsequently move toward Iceland or into Baffin Bay. Migration of systems from Baffin Bay across Greenland is rare due to orographic blocking (Putnins, 1970), although inspection of the daily NMC SLP charts reveals that deep systems do occasionally cross the lower southern section of the ice sheet.

It has often been suggested that through enhancing low-level temperature contrasts, cyclonic activity will be influenced by the distribution of sea ice and open water (e.g., Overland and Pease, 1982; Carleton, 1985). The cyclogenetic region shown by Whittaker and Horn (1984) near Svalbard, along the mean maximum winter sea ice margin, may reflect such a local effect. Furthermore, as indicated previously, events of cyclone intensification in the Greenland and Norwegian seas can sometimes be linked to temperature advection in which the open water-sea ice distribution must play an important role (U.K. Meteorological Office, 1964). Although a comparison between Figs. 1 and 4 also suggests a tendency for eastern Arctic cyclones to parallel the ice edge, this does not necessarily imply a sea ice-to-atmosphere forcing. Indeed, from the viewpoint that baroclinic disturbances will tend to be steered by upper-level longwave flow, the general ENE track of eastern Arctic cyclones (as well as the general cyclone frequency maximum in this region) is consistent with the position and orientation of the eastern limb of the mean North American 500 mb trough (Palmen and Newton, 1969). The open water-sea ice distribution will also, to some extent, tend to be controlled by the effects of cyclonic activity.

The distributions of cyclone and anticyclone activity and system pressures are closely related to the mean winter SLP field. The mean field (Fig. 5) shows closed mean high pressure centers over eastern Siberia (1028 mb) and Alaska/Yukon (1020 mb), and a strong trough over the eastern Arctic, with pressures decreasing to 1002 mb near Iceland. A weaker trough is located over Baffin Bay, separated from the eastern Arctic trough by a mean ridge over Greenland. The closed highs over Siberia and Alaska/Yukon correspond to the anticyclone frequency maxima in these

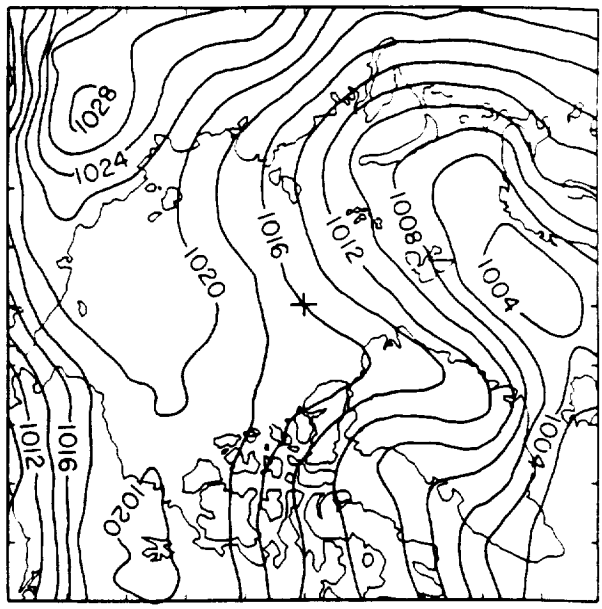

Fig. 5. Mean SLP field (mb) for winter from NMC analyses, 1952/53–1988/89

regions. The higher pressure on the Eurasian side, while to some extent likely biased due to the sea level correction problem described earlier, is also consistent with more frequent anticyclones in this region. The eastern Arctic and Baffin Bay troughs correspond to the frequent cyclonic activity in these regions, with the lowest pressures found near Iceland where, of course, the cyclones are most frequent and deepest.

3.2 Summer

During summer, cyclones are still most frequent near Iceland, the eastern Arctic and Baffin Bay, but with lower peak values than for winter (Fig. 6a). The primary difference from winter is that cyclones are distributed more widely throughout the Arctic. In particular, prominent frequency peaks are now found over the Alaska/Yukon region ($>9\%$), and western Eurasia ($>5\%$), with frequencies $>3\%$ also found over a broad region over Siberia. Frequencies $>3\%$ are found over a broad region in the central Arctic Ocean extending to the pole. While these results, in general, agree well with those of earlier studies, Whittaker and Horn (1984) show no local peak in cyclonic activity over the central Arctic, but rather a general increase from winter over the entire Arctic Ocean. This may simply reflect the larger scale of their

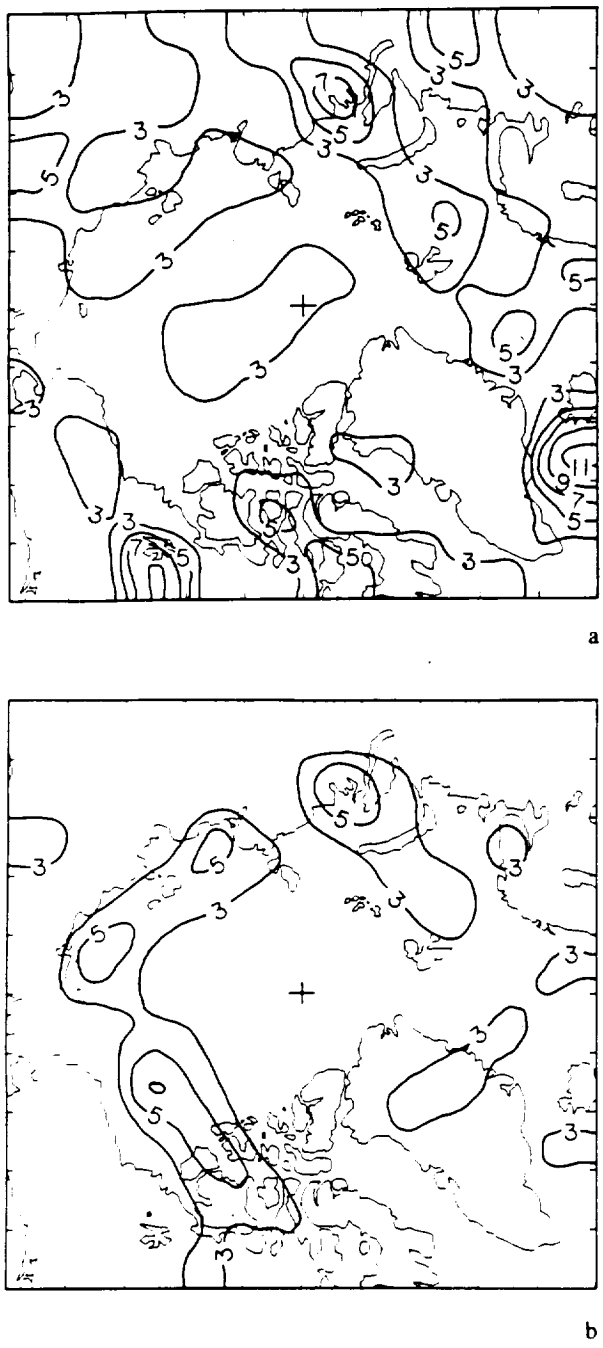

Fig. 6. Cyclone (a) and anticyclone (b) °$_0$ frequencies for summer, 1952–1989 in squares of 306,000 km^2 for systems with central pressure < 1012 mb (cyclones) and > 1012 mb (anticyclones). A cutoff contour of 3°$_0$ frequency is chosen to accentuate areas of frequent synoptic activity

analysis, in which the more frequent cyclonic systems is southerly latitudes act of dominate the map patterns.

There are also marked changes in the distribution of anticyclones (Fig. 6b). While a frequency maximum is still shown over Greenland, the Siberian and Alaska/Yukon peaks are no longer present. By contrast, anticyclonic activity has increased over the Kara, Laptev, East Siberian and Beaufort seas, and extending into the Canadian

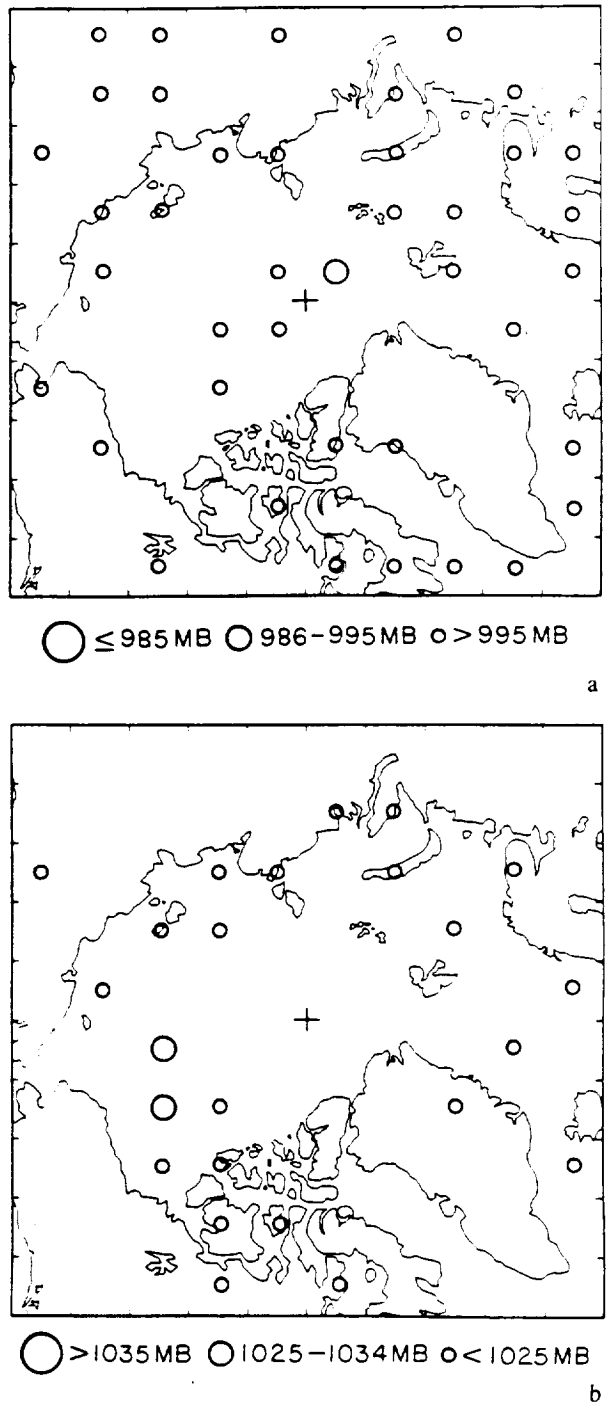

Fig. 7. Mean cyclone (a) and anticyclone (b) pressures (mb) for summer, 1952–1989 for grid cells with >3°$_0$ frequency of cyclones

Arctic Archipelago, forming a distinct "cellular" pattern also noted in earlier studies (Reed and Kunkel, 1960; Serreze and Barry, 1988).

Figure 7a shows that during summer, there is little spatial variability in mean central cyclone pressures, with all but one cell near the pole having mean pressures >995 mb. In particular, in the eastern Arctic, mean pressures are typically 10 mb higher than those observed for winter. Summer anticyclones (Fig. 7b) also tend to be considerably weaker than their winter counterparts, with systems over most grid cells having central pressures of <1025 mb. Anticyclones over the Beaufort Sea tend to be strongest, with central pressures from 1025–1034 mb.

Figure 8, showing mean cyclone tracks for summer prepared from the 15-year analysis (again only for cells with at least a 3% frequency of cyclones) indicates that as for winter, the Barents and Norwegian seas are common entrance zones for systems migrating into the Arctic, with systems taking an ENE track. Cyclone motion over Baffin Bay is also similar to winter. In contrast, however, some systems tend to parallel the Eurasian coast,

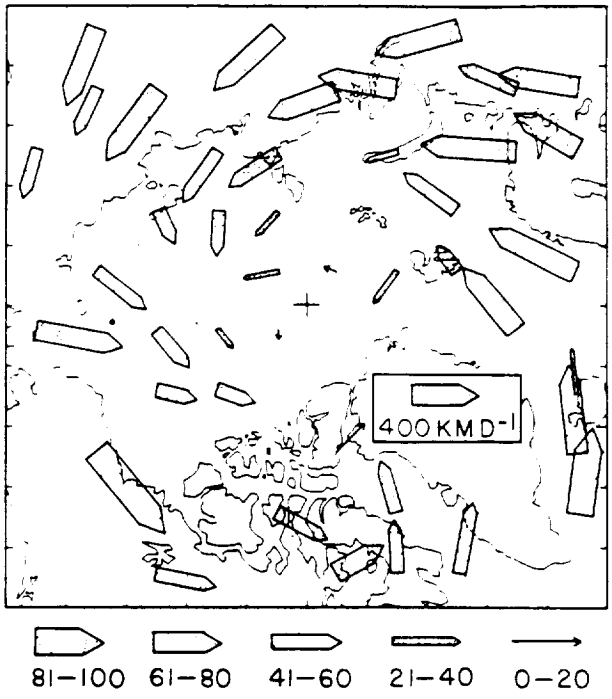

Fig. 8. Mean cyclone motion vectors for summer, 1975–1989. The length of each arrow is the mean vector magnitude, with the width proportional to the index of motion constancy, V_r/V_s (see text). Vectors are only plotted for grid cells with at least a 3% frequency of cyclones

with others migrating into the Arctic Ocean along a broad zone from the Laptev Sea eastward to the Chukchi Sea. Systems found within the central Arctic Ocean tend to stall, as shown by small magnitude of the velocity vectors and low constancy values. Eastward-migrating systems are also found along the Canadian Arctic Archipelago and over Alaska. These tracks are in good agreement with those shown by Whittaker and Horn (1984) for July, particularly with respect to motion parallel to the Eurasian and North American coasts, and the tendency for the Laptev, East Siberian and Chukchi seas to be common zones of migration into the Arctic Ocean. A tendency for systems to enter the Arctic from the Laptev Sea is also noted by Gorshkov (1983). Barry et al. (1987) remark on this pattern as having pronounced influence on Arctic cloud cover during late spring and early summer.

Earlier studies have shown that during summer, an Arctic frontal zone, separate from the Polar front, can be identified over northern Eurasia (Krebs and Barry, 1970), and southeastward across Canada (Bryson, 1966; Barry, 1967). While Reed and Kunkel (1960) consider the front to arise primarily from heating contrasts along the land/ocean boundary, the analyses referred to above find that it tends to be found along the boreal forest/tundra boundary, or ecotone (Hare, 1968), apparently as a result of contrasts in net radiation, evaporation fluxes and surface roughness. Because of its complex behavior, other factors, such as orography, are likely also involved (Reed and Kunkel, 1960).

The results from Whittaker and Horn (1984) suggest that cyclogenesis occurs in preferred regions along the Arctic front. As in winter, Arctic cyclones frequently originate along the mid-Atlantic seaboard (less active than in winter), east of Labrador and southern Greenland, but additional regions of cyclogenesis are indicated over southern Scandinavia, within two small areas approximately bounded by 60°–62° N latitude and 90°–110° E longitude, south of the Taymyr Peninsula, and two larger regions bounded by approximately 62–68° N latitude and from 130°–140° E and 150°–160° E over eastern Siberia. On the North American side, the cyclogenetic region east of the Rockies observed in winter is shown extending nearly to the Arctic Ocean coast; this can be associated with the cyclone maximum in

this region shown in Fig. 6a. Cyclogenesis is also indicated in a narrow region from Hudson Bay northward to Baffin Island, in turn associated with a summer cyclone frequency maximum.

The cyclone maximum over the central Arctic Ocean is of particular interest in that in many years, it may reflect a persistent low in monthly SLP fields during summer (Serreze and Barry, 1988) in turn associated with temporary reversals of the mean clockwise ice motion in the Beaufort Gyre (Serreze et al., 1989). Divergence of sea ice beneath the low pressure area may force the development of open water in the pack ice (Hibler, 1974; Serreze et al., 1989). The cyclones comprising this maximum originate primarily from Eurasia, and are typically mature or decaying (LeDrew, 1983). The constant influx of systems propagating around the periphery of the existing low tends to maintain a barotropic "cold low" structure (Reed and Kunkel, 1960) sometimes persisting for a month or more (Serreze and Barry, 1988). However, LeDrew et al. (1991) identify several additional factors that may tend to maintain the pattern. These include enthalpy fluxes associated with open water areas in the pack ice (suggesting a possible feedback between cyclonic activity and sea ice divergence), as well as an increase in available isentropic potential vorticity, related to a seasonal transition toward a more vigorous winter polar vortex.

The summer absence of a Siberian anticyclone center can be understood in terms of the positive surface radiation budget driven by the strong solar flux and snow-free surface. The disappearance of the Alaska/Yukon anticyclone peak is presumably in part related to the same effect (Keegan, 1958), although the weaker 500 mb ridge over this region observed in summer would also lessen the tendency for blocking-type Pacific highs. Nevertheless, Bell and Bosart (1989) show this region to remain as a local maximum of 500 mb closed highs.

With regard to the "cellular" pattern of peak summer anticyclone frequencies (Fig. 6b), Gorshkov (1983) shows that summer anticyclones tend to form in the eastern Arctic, particularly near Svalbard and the Kola Peninsula, and migrate eastward along the Eurasian marginal seas into the Beaufort Sea and the Canadian Arctic Archipelago. Along this general track, anticyclogenesis is indicated in the Beaufort Sea during June and near the Taymyr Peninsula in August, a pattern which seems broadly consistent with the results in Fig. 6b. Comparison between Figs. 6a and 6b shows that for the Kara Sea, the region extending from the Laptev to the East Siberian Sea, and in the eastern Canadian Arctic Archipelago, anticyclones and cyclones are both common; the implied alternation between synoptic regimes being indicative of the frequent passage of baroclinic waves.

It is useful again to examine relationships between synoptic activity and the mean summer SLP distribution. The mean SLP distribution for summer (Fig. 9) tends to be flat. This can be interpreted as resulting from a more even distribution of cyclonic activity than observed in winter, the general lack of spatial variations in mean cyclone and anticyclone pressures, as well as the tendency in other regions for alternation between cyclonic and anticyclonic regimes. Perhaps the only notable features of the mean summer SLP pattern are the weak mean high pressure cell over the Beaufort Sea, which corresponds to the region of both the highest frequency of anticyclonic activity and the strongest systems, and the weak pressure trough over eastern Siberia, which can be related to the broad cyclone frequency maximum in this region. The lack of a mean summer low in the central Arctic does not

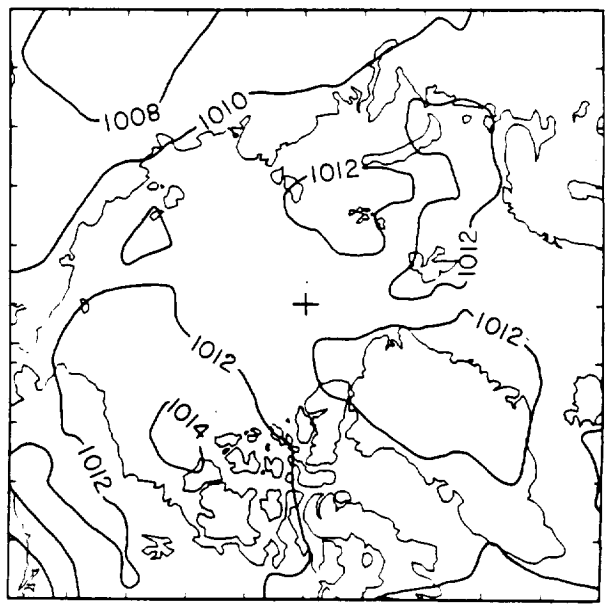

Fig. 9. Mean summer SLP field (mb) from NMC analyses, 1952–1989

contradict earlier discussion concerning the effects of the central Arctic cyclone pattern. Over individual years, the timing of peak cyclonic activity can occur as early as June and as late as September (Serreze and Barry, 1988). This variability is masked by the use of a three month average.

3.3 *Annual Cycle of Synoptic Activity*

A basic feature of the Arctic circulation that GCMs should be able to reproduce is the annual cycle of Arctic synoptic activity, since this represents the most basic form of climatic response to changes in seasonal forcing. We have calculated mean monthly cyclone and anticyclone central pressures and the mean normalized number of systems with their respective standard deviations, based on all systems found above 65° N over the 1952–1989 record. The monthly mean system counts are normalized to account for occasional missing days in the NMC pressure record. As we are dealing with a single large area, expressing synoptic activity in terms of systems per month seems more straightforward than using percent frequency values. Results are shown in Table 1.

There is a strong annual cycle in both cyclone and anticyclone mean pressures. Cyclone pressures show a range of 10 mb from a minimum of 990 mb in December to 1000 mb during May. The standard deviation in mean cyclone pressures also tends to be greater during the winter months, peaking in February (5.2 mb), with a minimum during June and July (1.6 mb). A strong annual cycle is also seen for anticyclone mean pressures ranging from 1034 mb in February to 1022 mb in July. Standard deviations show a similar seasonal cycle, being largest in January (5.1 mb) and smallest during June and July (1.5 mb).

Cyclone and anticyclone occurrence also exhibits a distinct seasonal cycle. Cyclones are least numerous during February (43 systems per month), rising to 64 systems per month in August, nearly a 50% increase. A pronounced increase in mean cyclone numbers is observed between April (46 systems) and June (63 systems). Interestingly, Huschke (1969) shows that for the central Arctic, the frequency of low-level Arctic stratus clouds also shows a sharp increase during this period, from 35% (April) to 90% (June), in turn associated with a sharp decrease in the frequency of surface-based temperature inversions over both land and ocean areas (Bilello, 1966; Serreze et al., 1992). The sharp increase in cyclonic activity between May (50 systems) and June (63 systems) also corresponds to the onset of widespread snow melt over the Arctic Ocean sea ice cover (Robinson et al., 1992).

Interestingly, anticyclones are shown to be least numerous in winter. This can be explained in that selecting only systems above 65° N excludes the strong wintertime Siberian and Alaska Yukon anticyclone centers; the summer peak reflects the effects of the increase in anticyclonic activity over the Arctic Ocean. There is no marked indication of a seasonal cycle in the standard deviation of either mean cyclone or anticyclone numbers; a value of 8–10 is typical for both systems.

Table 1. *Seasonal Cycle in Cyclone (C) and Anticyclone (AC) Mean Central Pressures and Normalized System Counts for the Region* > 65° N. Values in parentheses are standard deviations (see text)

	Mean Pressure (mb)		Normalized Counts	
	Cyclones	Anticyclones	Cyclones	Anticyclones
Jan.	992 (4.8)	1033 (5.1)	49 (10)	45 (8)
Feb.	993 (5.2)	1034 (4.3)	43 (10)	42 (10)
Mar.	994 (4.8)	1033 (4.7)	47 (11)	49 (9)
Apr.	998 (2.7)	1031 (2.8)	46 (10)	51 (10)
May	1000 (1.9)	1029 (2.7)	50 (12)	57 (9)
Jun.	999 (1.6)	1023 (1.5)	63 (13)	53 (8)
Jul.	999 (1.6)	1022 (1.5)	62 (10)	55 (8)
Aug.	998 (2.1)	1023 (1.9)	64 (13)	49 (8)
Sep.	995 (3.0)	1024 (1.8)	61 (8)	44 (8)
Oct.	993 (3.5)	1026 (3.1)	62 (10)	44 (10)
Nov.	992 (3.5)	1030 (2.9)	52 (11)	46 (8)
Dec.	990 (4.9)	1031 (4.2)	54 (10)	45 (9)

North of 65° N, cyclones outnumber anticyclones in all months except March through May, when anticyclones are slightly more numerous. While a direct comparison of the results in Table 1 is difficult in that a 1.5 mb threshold is used to identify anticyclones, as opposed to 2 mb for cyclones (see section 2b), we find that during spring, anticyclonic activity decreases sharply over both Alaska/Yukon (up to an 8% frequency reduction) and Siberia (up to a 12% frequency reduction), but increases slightly over the Beaufort Sea (+ 1–3% frequency increase). As shown by Walsh and Chapman (1990), the mean Beaufort Sea high (and hence the clockwise Beaufort Gyre sea ice circulation depicted in Fig. 1) is in turn most pronounced during this season.

4. Time Series of Synoptic Activity

To examine possible temporal trends in synoptic activity, seasonal time series of cyclone and anticyclone mean central pressures and the normalized number of systems were compiled based on all systems above 65° N. Using a linear least squares (LLS) regression, a regression slope (β_1) was first computed for each full time series, with the statistical significance of each slope determined from a 2-tailed Student's t-test. As the computed regression slopes can be sensitive to the influence of outliers, especially at the end points, the regression analyses were then run an additional three times, eliminating the beginning, final and both endpoints. Only those slopes passing the t-test at the 0.05 level from all four runs are considered to be significant. As a further check on the influence of outliers, β_1 slopes were calculated using a least absolute deviation (LAD) estimation (e.g., Barrodale and Roberts, 1974), which differs from LLS in that instead of minimizing the sum of the squared differences between the observed and predicted values of the dependent variable (y_i and $\langle y \rangle_i$ respectively) over the N observations, one minimizes the summed values

Table 2. *Results from Trend Analysis of Cyclone (C) and Anticyclone (AC) Mean Pressures (mb) for the Region > 65° N.* Values in parentheses are the least absolute deviation slopes (see text)

		Winter	Spring	Summer	Autumn
N		37	38	37	37
β_1 (mb/yr)	C	−0.108 (−0.056)	−0.023 (−0.031)	+0.010 (+0.038)	−0.019 (0.000)
	AC	−0.033 (−0.067)	−0.040 (−0.095)	+0.008 (0.000)	+0.043 (+0.043)
β_1*N (mb)	C	−4.01 (−2.07)	−0.87 (−1.18)	+0.37 (+1.41)	−0.71 (0.00)
	AC	−1.22 (−2.48)	−1.53 (−3.61)	+0.29 (0.00)	+1.58 (+1.59)
Mean (mb)	C	991	997	998	993
	AC	1033	1031	1023	1027
S.D. (mb)	C	3.5	2.1	1.3	2.3
	AC	3.0	2.0	1.1	1.8

Table 3. *Results from Trend Analysis of Cyclone (C) and Anticyclone (AC) Normalized System Counts for the Region > 65° N.* Underlined slopes are significant at the 0.05 probability level. Values in parentheses are the least absolute deviation slopes (see text)

		Winter	Spring	Summer	Autumn
N		37	38	37	37
β_1 (syst./yr)	C	+0.882 (+0.893)	+0.858 (+1.000)	+1.154 (+1.133)	+0.439 (+0.533)
	AC	+0.246 (+0.522)	+0.693 (+0.815)	+1.057 (+1.000)	+0.705 (+0.700)
β_1*N (syst.)	C	+32.6 (+33.0)	+32.6 (+38.0)	+42.7 (+41.9)	+16.2 (+19.7)
	AC	+9.1 (+19.3)	+26.3 (+31.0)	+39.1 (+37.0)	+26.1 (+25.9)
Mean (syst.)	C	146	143	188	176
	AC	133	158	157	134
S.D. (syst.)	C	21.0	21.1	22.5	20.0
	AC	22.6	21.9	17.5	19.9

of $|y_i - \langle y \rangle_i|$. It is through elimination of the squaring procedure that the sensitivity to outliers is reduced.

Results from the trend analyses are summarized in Tables 2 and 3, which, for cyclones (C) and anticyclones (AC), lists for each full time series the number of years (N) used in the regression analysis, and from both the LLS and LAD analyses (the latter in parentheses) the β_1 slopes, and the cumulative change over the period of record (β_1*N). The mean and standard deviation (S.D.) of each time series are also given. Those LLS β_1 slopes determined to be significant at the 0.05 level from the four runs described above are underlined.

The results from the LLS analysis show no significant trends in cyclone or anticyclone mean pressures (Table 2). By contrast, significant positive trends are found for cyclone numbers for winter, spring and summer, and for anticyclone

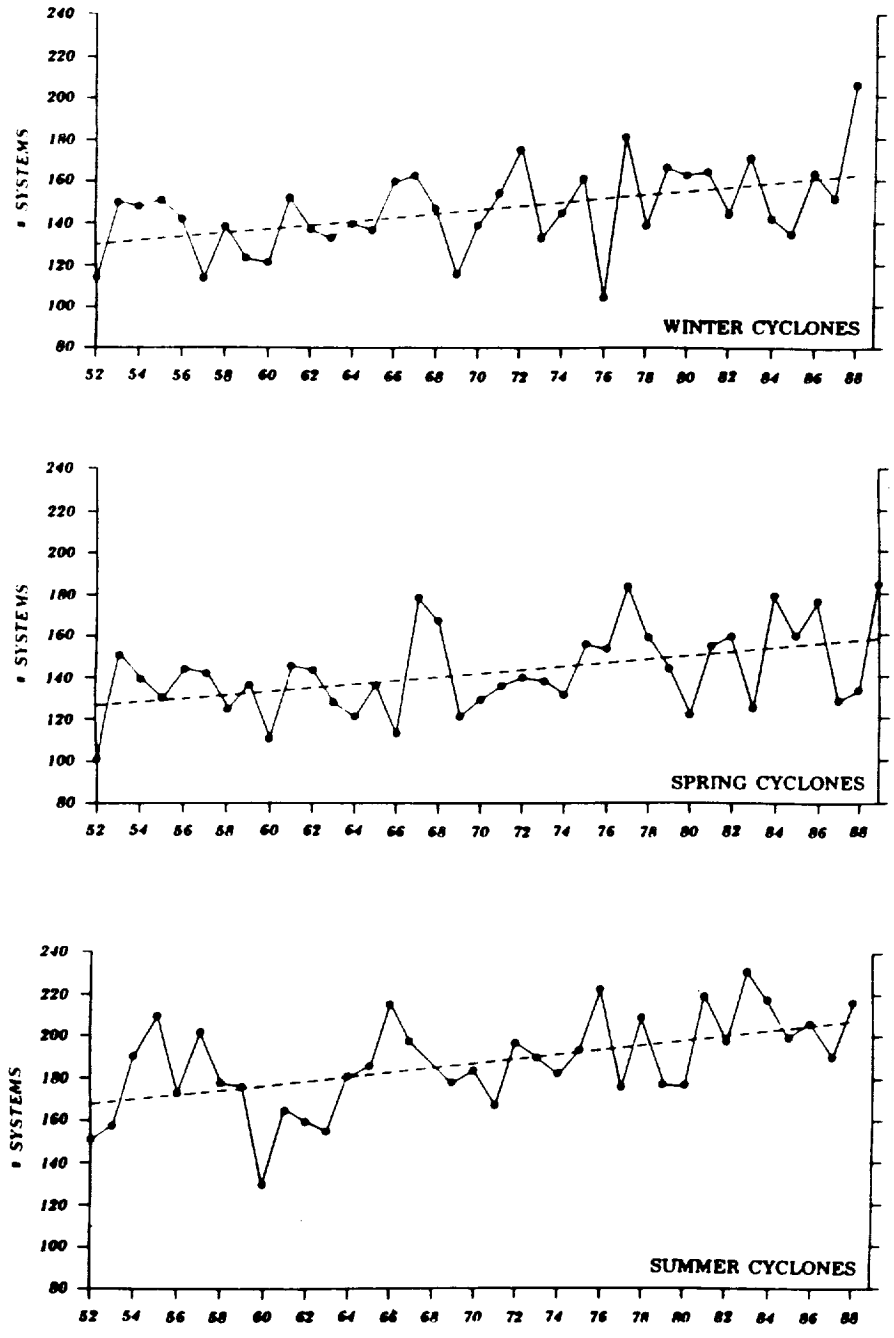

Fig. 10. Times series of cyclone counts north of 65° N for winter, spring and summer. The linear least squares regression slopes (see text) are indicated by dashed lines

numbers during spring, summer and autumn (Table 3). The trends in both cyclone and anticyclone numbers are largest during summer, with LLS slopes (systems/year) of + 1.154 (cyclones) and + 1.057 (anticyclones), yielding estimated increases in cyclone and anticyclone counts over the period of record of 43 and 39 systems, respectively. Note that the significant LLS slopes in Table 3 and the corresponding LAD slopes agree well in magnitude, increasing our confidence in the LLS estimates. The seasonal time series of cyclone and anticyclone counts shown as significant from the LLS regressions are given in Figs. 10 and 11.

Do the results in Figs. 10 and 11 indicate a true change toward increased synoptic activity? The biggest unknown regards the quality of the SLP data (see section 2.1). Intuitively, one would expect that as the observing network improves, there will be a tendency for more cyclones and

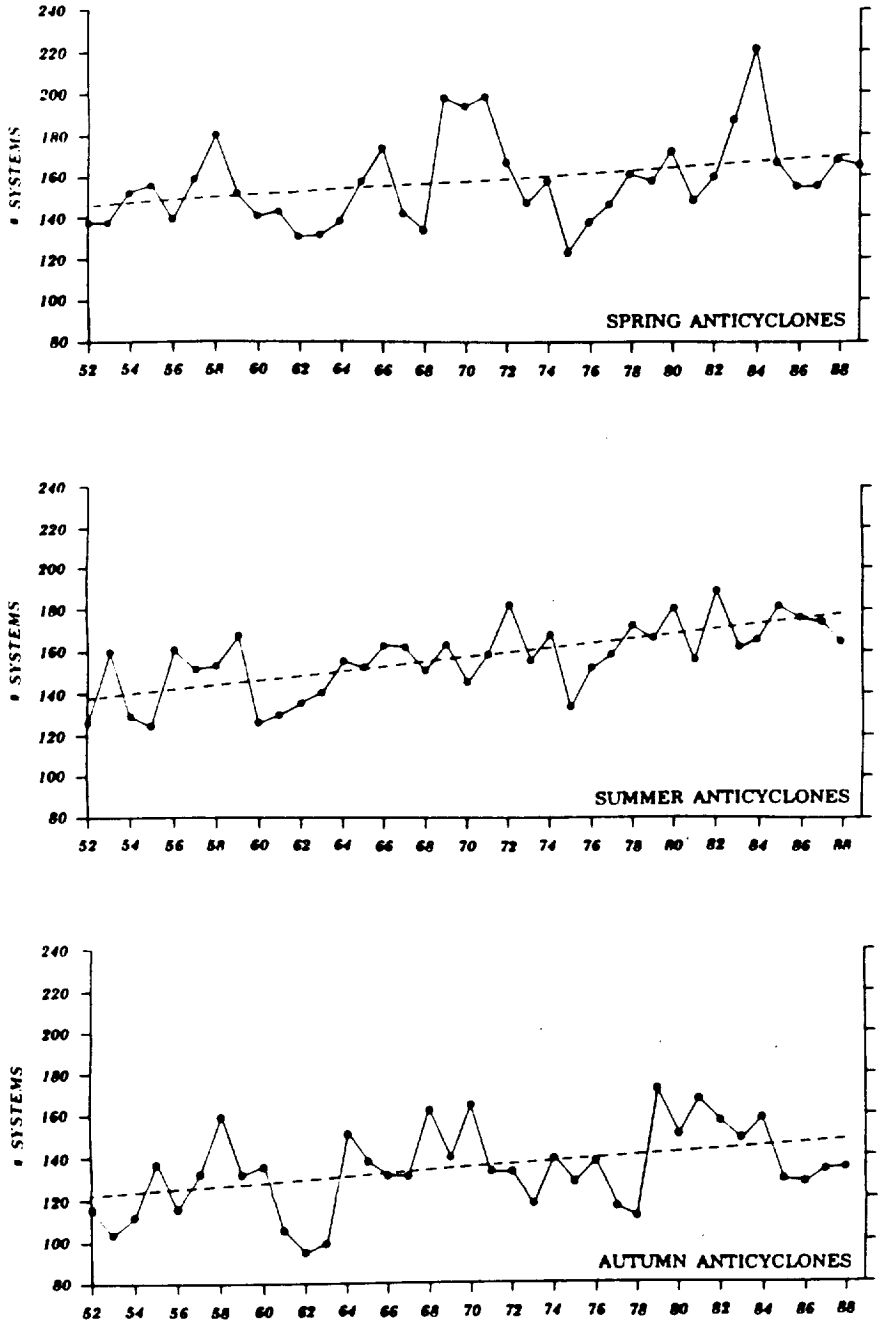

Fig. 11. Time series of anticyclone counts north of 65° N for spring, summer and autumn. The linear least squares regression slopes (see text) are indicated by dashed lines

anticyclones to be captured in the analyses. On this basis, we might expect a "step" in system numbers after 1962 when the NMC final analyses began to be archived, or after 1978, when AOBP buoy data over the Arctic Ocean began to be included in the NMC analyses, but this is not observed. Indeed, some of the highest system counts are observed in the earlier part of the records.

Based on rawinsonde data from a network of coastal stations, Bradley et al. (in press) identify a systematic reduction in the depth of surface-based wintertime temperature inversions in recent decades, with accompanying increases in mean surface temperature. While they argue that this could reflect several factors, including increases in warm air advection, ice crystals, aerosols or greenhouse gases, these changes in inversion characteristics could reflect the effects of increased cyclonic activity during this season, which, by advection, mechanical mixing, or through the effects on the longwave budget forced by increased cloud cover and water vapor, could increase surface temperatures and erode the inversion layer. Chapman and Walsh (1993) find that the increase in surface air temperatures is primarily a winter and spring phenomenon, restricted to land areas. While again, these temperature changes might result from increased synoptic activity, it is also possible that they represent a mechanism by which baroclinicity and eddy frequency could increase, at least for these seasons.

5. Summary and Conclusions

Characteristics of Arctic synoptic activity are examined for 1952–1989 using gridded NMC SLP fields. The main conclusions are summarized as follows:

1) During winter, cyclonic activity tends to be most common near Iceland, the eastern Arctic, Baffin Bay, and the southern Canadian Arctic Archipelago. Cyclones tend to be deepest near Iceland, the Norwegian Sea and west of southern Greenland. Most winter cyclones enter the Arctic Ocean from along the Greenland and Norwegian seas and track ENE, tending to fill as they approach the Kara Sea. These systems have their origins in mid-latitude cyclogenetic regions, as well as locally in the eastern Arctic and sub-arctic seas.
2) Winter anticyclones are most common over eastern Siberia, Alaska/Yukon and a broad area over the central Arctic Ocean. Earlier studies show that while the Siberian and Arctic Ocean anticyclones are typically shallow, cold systems, those over Alaska/Yukon include Pacific blocking systems, as well as systems imported from lower latitudes.
3) During summer, cyclonic activity remains common in the same regions as observed for winter. Cyclonic activity increases over northern Eurasia and North America, with systems entering the Arctic Ocean along a broad entrance zone from the Laptev Sea eastward to the Chukchi Sea. Cyclogenesis occurs in several preferred areas over northern Eurasia and Canada.
4) The winter anticyclone centers over Siberia and Alaska/Yukon disappear during summer, and are replaced by new centers of activity over the Kara, Laptev, East Siberian and Beaufort seas, and the Canadian Arctic Archipelago. Except for the Beaufort Sea, regions of frequent cyclonic activity over the ocean overlap those of anticyclonic activity.
5) Summer cyclones and anticyclones are considerably weaker than their winter counterparts.
6) The seasonal distribution of synoptic activity shows a strong relationship with mean SLP fields. Peak strength of the Beaufort Gyre ice circulation during spring can be related to a seasonal shift toward increased anticyclonic activity over the Beaufort Sea, at which time anticyclonic activity over Alaska/Yukon and Siberia is rapidly decreasing.
7) For the Arctic above 65° N, cyclone and anticyclone activity exhibits a strong annual cycle, with both cyclones and anticyclones being least numerous, but strongest, during the winter months. Cyclonic activity above 65° N exhibits a sharp increase between April and June, which, in turn, is associated with a sharp increase in the extent of low-level Arctic stratus, and a sharp decrease in the frequency of surface-based temperature inversions. Increased cyclonic activity during May and June also corresponds to the timing of widespread snow melt over the sea ice cover.
8) For the region above 65° N, LLS analyses reveal that since 1952, cyclone numbers have

increased during winter, spring and summer, while anticyclone numbers have increased during spring, summer and autumn. While these trends may simply reflect the effects of improvement over time of the SLP analyses, they may represent a true climatic shift. One way to address this issue would be to use rawinsonde data for Arctic stations above 65° N to examine whether there have been any changes in the variance of lower-tropospheric heights, as this could provide an independent index of synoptic activity. It would also be interesting to examine the results of GCM transient experiments where greenhouse gas concentrations are steadily increased, to see if any corresponding modeled trends in synoptic activity are apparent in the Arctic.

Acknowledgements

This study was supported by the National Science Foundation under grants NSF/DPP-9214838 and NSF/DPP-9113673, by EPRI (RP2333-07), NASA (NAGW-2407) through a University of Washington subcontract, and the CIRES CCHE undergraduate internship program. The NSIDC computer staff is thanked for systems support and Tim Brown (CIRES) for performing the trend analyses. We also thank the reviewers for their helpful comments.

References

Barrodale, I., Roberts, F. D. K., 1974: Algorithm 478. Solution of an overdetermined system of equations in the L_1 norm. *Commun. A.C.M.*, **7**, 319–320.

Barry, R. G., 1967: Seasonal location of the Arctic front over North America. *Geogr. Bull.*, **9**, 79–95.

Barry, R. G., Crane, R. G., Schweiger, A., Newell, J., 1987: Arctic cloudiness in spring from satellite imagery. *J. Climatol.*, **7**, 423–451.

Bell, G. D., Bosart, L. F., 1989: A 15-year climatology of Northern Hemisphere 500 mb closed cyclone and anticyclone centers. *Mon. Wea. Rev.*, **117**, 2142–2163.

Bilello, M. A., 1966: Survey of Arctic and Subarctic temperature inversions. *Tech Rep. 161*, Cold Regions Res. and Eng. Lab., Hanover, N.H., 36 pp.

Borisov, A. A., 1965: *Climates of the U.S.S.R.*, Edinburgh: Oliver and Boyd, 255 pp.

Bradley, R. S., England, J., 1979: Synoptic climatology of the Canadian High Arctic. *Geografiska Annaler*, **61A**, 187–201.

Bradley, R. S., Keimig, F. T., Diaz, H. F., 1993: Recent changes in the north American Arctic boundary layer in winter. *J. Geophys. Res.* (in press).

Bryson, R. A., 1966: Air masses, streamlines and the boreal forest. *Geogr. Bull.*, **8**, 228–269.

Carleton, A. M., 1985: Synoptic cryosphere–atmosphere interactions in the northern hemisphere from DMSP image analysis. *Int. J. Remote Sensing*, **6**, 239–261.

Chapman, W., Walsh, J. E., 1993: Recent variations of sea and air temperatures at high latitudes. *Bull. Amer. Meteor. Soc.*, **74**(1), 33–47.

Cubasch, U., Cess, R. D., 1990: Processes and modeling. In Houghton, J. T., Jenkins, G. J., Ephraumus, J. J. (eds.) *Climate Change. The IPCC Scientific Assessment*. Cambridge: Cambridge University Press, 364 pp.

Dickson, R. R., Meincke, J., Marlberg, S. A., Lee, A. J., 1988: The "Great Salinity Anomaly" of the northern North Atlantic, 1968–1982. *Prog. Oceanogr.*, **20**, 103–151.

Dorsey, H. G., Jr., 1945: Some meteorological aspects of the Greenland Ice Cap. *J. Meteor.*, **2**, 135–142.

Dzerdzeevskii, B. L., 1945: Tsirkuliatsionnye skhemy v troposfere Tsentralnoi Arktiki. *Izdatel'stvo Akademii Nauk*, 28 pp. (English translation in Scientific Report No. 3 under Contract AF19(122)-228, Meteorology Department, UCLA).

Gorshkov, S. G., 1983: *World Ocean Atlas Vol. 3 Arctic Ocean*. New York: Pergamon Press, 184 pp.

Hansen, J., Lebedeff, S., 1987: Global trends of measured surface air temperature. *J. Geophys. Res.*, **92**, 13345–13372.

Hare, F. K., 1968: The Arctic. *Quart. J. Roy. Meteor. Soc.*, **94**, 439–459.

Hare, F. K., Orvig, S., 1958: The arctic circulation: a preliminary view. Arctic Meteorology Research Group Publication in Meteorology, No. 12. Montreal: McGill University, 211 pp.

Hastings, A. D., 1971: Surface climate of the Arctic basin. Report ETL-TR-71-5, U.S. Army Engineer Topographic Laboratories, Fort Belvoir, VA, 98 pp.

Hayden, B. P., 1981a: Secular variation in Atlantic coast extratropical cyclones. *Mon. Wea. Rev.*, **109**, 159–167.

Hayden, B. P., 1981b: Cyclone occurrence mapping: equal area or raw frequencies? *Mon. Wea. Rev.*, **109**, 168–172.

Helmholtz, H. von, 1888: Über atmosphärische Bewegungen. *Meteor. Zeit.*, **5**, 329–340.

Hibler, W. D. III, 1974: Differential sea ice drift II. Comparisons of mesoscale strain measurements to linear drift theory predictions. *J. Glaciol.*, **13(69)**, 457–471.

Hobbs, W. H., 1910: Characteristics of the inland ice of the Arctic regions. *Amer. Phil. Soc.*, **49**, 57–129.

Hobbs, W. H., 1926: *The Glacial Anticyclones, the Poles of the Atmospheric Circulation*. New York: MacMillan, 198 pp.

Hobbs, W. H., 1945: The Greenland glacial anticyclone. *J. Meteor.*, **2**, 143–153.

Huschke, R. E., 1969: Arctic cloud statistics from "air-calibrated surface weather observations", United States Air Force Project Rand Contract Number F44620-67-C-0015.

Jones, P. D., 1987: The twentieth century Arctic high-fact or fiction? *Clim. Dynam.*, **1**, 63–75.

Keegan, T. J., 1958: Arctic synoptic activity in winter. *J. Meteor.*, **15**, 513–521.

Krebs, S. J., Barry, R. G., 1970: The arctic front and the tundra-taiga boundary. *Geogr. Rev.*, **60**, 548–554.

LeDrew, E. F., 1983: Dynamic climatology of the Beaufort to Laptev Sea sector of the polar basin for the summers of 1975 and 1976. *J. Climate Appl. Meteor.*, **3**, 335–359.

LeDrew, E. F., 1984: The role of local heat sources in synoptic activity in the Arctic Basin. *Atmos. Ocean*, **22**, 309–327.

LeDrew, E. F., 1987: Development processes for five depression systems within the Polar Basin. *J. Climate Appl. Meteor.*, **8**, 125–153.

LeDrew, E. F., Johnson, D., Maslanik, J. A., 1991: An examination of atmospheric mechanisms that may be responsible for the annual reversal of the Beaufort Gyre sea ice fields. *Int. J. Climatology*, **11**, 841–859.

Loewe, F., 1936: The Greenland ice cap as seen by a meteorologist. *Quart. J. Roy. Meteor. Soc.*, **62**, 359–377.

Mass, C., Edmon, H., 1987: *Compact Disk of the National Meteorological Center Grid Point Data Set, General Information and User's Guide*. Seattle: Dept. Atmos. Sci., Univ. Washington, 11 pp.

Matthes, F. E., 1946: The glacial anticyclone theory examined in light of recent meteorological data from Greenland, Part I. *Trans. Amer. Geophys. Union*, **27**, 324–341.

Matthes, F. E., Belmont, A. D., 1946: The glacial anticyclone theory examined in light of recent meteorological data from Greenland, Part II. *Trans Amer. Geophys. Union*, **31**, 174–182.

Namias, J., 1958: The general circulation of the lower troposphere over Arctic regions and its relation to the general circulation elsewhere. *Polar Atmosphere Symposium, Part I, Meteorology Section*. New York: Pergamon Press, 45–61.

Overland, J. E., Pease, C. H., 1982: Cyclone climatology of the Bering Sea and its relation to sea ice extent. *Mon. Wea. Rev.*, **110**(1), 5–13.

Palmen, E., Newton, C. W., 1969: *Atmospheric Circulation Systems*. New York: Academic Press, 603 pp.

Pettersen, S., 1950: Some aspects of the general circulation of the atmosphere. *Centenary Proc. of the Royal Meteorological Society*, London, 120–153.

Putnins, P., 1970: The climate of Greenland. In: Orvig, S. (ed.) *Climates of the Polar Regions* (World Survey of Climatology, vol. 14). Amsterdam: Elsevier, 3–124.

Rae, R. W., 1951: *The Climate of the Canadian Archipelago*. Toronto: Department of Transport, 90 pp.

Reed, R. J., Kunkel, B. A., 1960: The arctic circulation in summer. *J. Meteor.*, **17**, 489–506.

Robinson, D. A., Serreze, M. C., Barry, R. G., Scharfen, G., Kukla, G., 1992: Large-scale patterns and variability of snow melt and parameterized surface albedo in the Arctic Basin. *J. Climate*, **5**(10), 1109–1119.

Schlesinger, M. E. (ed.), 1988: *Physically Based Modeling and Simulation of Climate and Climate change*. Kluwer Academic, 1084 pp. (NATO ASI Series C, Vol. 243

Serreze, M. C., Barry, R. G., 1988: Synoptic activity in the Arctic Basin, 1979–85. *J. Climate*, **1**(12), 1276–1295.

Serreze, M. C., Barry, R. G., McLaren, A. S., 1989: Seasonal variations in sea ice motion and effects on sea ice concentration in the Canada Basin. *J. Geophys. Res.*, **94**, 10,955–10,970.

Serreze, M. C., Kahl, J. D., Schnell, R. C., 1992: Low-level temperature inversions of the Eurasian Arctic and comparisons with Soviet drifting station data. *J. Climate*, **5**(6), 615–629.

Sverdrup, H. U., 1983: *The Norwegian North Polar Expedition with the "Maud", 1918–1925, Volume II, Meteorology*. Bergen: John Griegs Boktrykkeri, 331 pp.

Taylor, K. E., 1986: An analysis of the biases in traditional cyclone frequency maps. *Mon. Wea. Rev.*, **114**, 1481–1490.

Thorndike, A. S., Colony, R., 1980: *Arctic Ocean Buoy Program Data Report, 1 January 1979–31 December 1979*. Polar Science Center, University of Washington, Seattle, 131 pp.

Trenberth, K. E., Olson, J. G., 1988: Evaluation of NMC global analyses: 1979–1987, *NCAR Technical Note*, NCAR/TN-299+STR, National Center for Atmospheric Research, Boulder, CO, 82 pp.

Trenberth, K. E., Paolino, D. A., 1980: The northern hemisphere sea level pressure data set: trends, errors and discontinuities. *Mon. Wea. Rev.*, **108**(7), 855–872.

U. K. Meteorological Office, 1964: *Weather in Home Fleet Waters. Volume I – The Northern Seas, Part 1*. London: Her Majesty's Stationery Office, 265 pp.

Walker, J. M., 1967: Subterranean isobars. *Weather*, **22**(7), 296–297.

Walsh, J. E., 1978: Spatial and temporal scales of the Arctic circulation. *Mon. Wea. Rev.*, **106**, 1532–1544.

Walsh, J. E., Chapman, W. L., 1990: Short-term climatic variability of the Arctic. *J. Climate*, **3**(2), 237–250.

Walsh, J. E., Crane, R. G., 1992: A comparison of GCM simulations of Arctic climate. *Geophys. Res. Lett.*, **19**, 29–32.

Walsh, J. E., Johnson, C. M., 1979: Interannual atmospheric variability and associated fluctuations in Arctic sea ice extent. *J. Geophys. Res.*, **34**, 6915–6928.

Washington, W. M., Meehl, G. A., 1989: Climate sensitivity due to increased CO_2: experiments with a coupled atmosphere and ocean general circulation model. *Clim. Dynam.*, **4**(1), 1–38.

Whittaker, L. M., Horn, L. H., 1984: Northern Hemisphere extratropical cyclone activity for four mid-season months. *J. Climatology*, **4**, 297–310.

Wilson, C. V., 1958: Synoptic regimes of the lower Arctic troposphere during 1955. *Arctic Meteorology Research Group, Publication in Meteorology* No. 8. Monteral: McGill University, 57 pp.

Zishka, K. M., Smith, P. J., 1980: The climatology of cyclones and anticyclones over North American and surrounding ocean environs for January and July, 1950–1977. *Mon. Wea. Rev.*, **108**, 387–401.

Authors' addresses: M. C. Serreze, J. E. Box, R. G. Barry, Cooperative Institute for Research in Environmental Sciences, University of Colorado, Boulder, CO 80309-0449, U.S.A. and J. E. Walsh, Department of Atmospheric Sciences, University of Illinois, Urbana-Champaign, Urbana, IL 61081, U.S.A.